

## Local band gap modulations in non-stoichiometric $V_2O_3$ films probed by scanning tunneling spectroscopy

V. Simic-Milosevic, N. Nilius,\* H.-P. Rust, and H.-J. Freund

*Department of Chemical Physics, Fritz-Haber-Institut der Max-Planck-Gesellschaft, Faradayweg 4-6, D-14195 Berlin, Germany*

(Received 7 September 2007; revised manuscript received 22 November 2007; published 11 March 2008)

Scanning tunneling microscopy and spectroscopy have been used to investigate the electronic structure of non-stoichiometric  $V_2O_3$  islands with a vanadyl termination grown on Au(111). The spectroscopic measurements reveal the correlation gap of bulk  $V_2O_3$  that varies between 0.2 and 0.75 eV for different sample preparations. In addition, gap modulations of roughly 0.2 eV are observed at different locations within the oxide islands. The changes in gap size are attributed to local deviations from the ideal  $V_2O_3$  stoichiometry in films produced at more oxidizing or reducing conditions. By evaluating the position of the Fermi level with respect to the band edges, a *p*-type conductance characteristic is dominantly observed for the  $V_2O_3$  islands, indicative of an efficient hole doping of the V 3*d* band.

DOI: [10.1103/PhysRevB.77.125112](https://doi.org/10.1103/PhysRevB.77.125112)

PACS number(s): 71.30.+h, 68.37.Ef, 73.61.Ng

### INTRODUCTION

The vanadium oxides form a fascinating class of materials that exhibit a large variety of structures with different physical and chemical properties. This diversity makes vanadium oxides technologically relevant and leads to various applications, such as in light detectors, write-erase media, electrical and optical switching devices, as well as in heterogeneous catalysis.<sup>1,2</sup> From the chemical point of view, the versatility of vanadium oxides is based on the large number of possible vanadium oxidation states ranging from  $V^{2+}$  to  $V^{5+}$  ( $VO$ ,  $V_2O_3$ ,  $VO_2$ , and  $V_2O_5$ ) as well as on the different oxygen coordination geometries occurring in the crystal structures. From a physical point of view, vanadia has attracted a lot of interest because of its rich electronic and magnetic structure and its phase transitions, in particular, the metal-insulator transition triggered by changes in temperature, doping level, and external pressure exerted on the oxide material.<sup>3</sup>

A particularly interesting example is vanadium sesquioxide ( $V_2O_3$ ), where the V atoms adopt an oxidation state of  $V^{3+}$  and a  $3d^2$  configuration. The oxide exhibits a metal-insulator transition (MIT) from a paramagnetic metal to an antiferromagnetic insulator at about 165 K.<sup>4</sup> At the transition temperature, the lattice symmetry changes from corundum to monoclinic, an energy gap opens in the local density of states (LDOS),<sup>5</sup> and the electric resistance increases by several orders of magnitude.<sup>6</sup> Information on the electronic structure of  $V_2O_3$  has been collected by means of photoemission and x-ray absorption spectroscopy, and revealed a Mott-Hubbard-type electronic characteristic and a strong hybridization between the O 2*p* and V 3*d* bands. The position of the O 2*p* valence band was determined to range from  $-4$  to  $-10$  eV, whereas the V 3*d* derived conduction band starts at approximately  $-3$  eV and exceeds the Fermi level.<sup>7,8</sup> However, the exact electronic structure of this material is still controversial.

Doping experiments with various cations, such as Ti, Cr, Fe, Zr, Al, and Mg, demonstrated the possibility of modifying the electronic properties of  $V_2O_3$ . It has been shown that the substitution of V by Ti stabilizes the metallic phase, while the insulating phase is supported by the other

substitutes.<sup>9-11</sup> The stabilization of the metallic phase was explained by enhanced orbital overlap and band broadening, caused by the larger spatial extension of the Ti 3*d* orbitals with respect to the V states.<sup>12</sup> Since the orbitals of the other cations are more contracted, they form localized states in the V 3*d* conduction band that favor an insulating character of  $V_2O_3$ . The MIT is also suppressed down to lowest temperatures in non-stoichiometric, hole-doped  $V_{2-y}O_3$  if the concentration of V vacancies is high enough (5%) to allow overlap between neighboring defect levels and formation of a defect band.<sup>13,14</sup> However, these studies did not provide direct insight into the band structure of  $V_2O_3$ , as the classification of electronic properties was only based on measurements of the electric resistance. The band gap of non-stoichiometric  $V_2O_3$  below the Mott transition depends strongly on the exact V to O ratio and was found to vary between 300 and 600 meV.<sup>15-18</sup> No information on spatial variations of the  $V_2O_3$  gap size and underlying fluctuations in the oxide stoichiometry are available so far.

In this study, we combine the unique capabilities of scanning tunneling microscopy (STM) to perform local topographic and electronic measurements to directly investigate the electronic structure of non-stoichiometric  $V_2O_3$  islands on Au(111) below the MIT. We will demonstrate that despite a perfectly crystalline surface structure, the electronic properties are not homogeneous within a particular oxide island, but vary on the length scale of 1 nm.

### EXPERIMENTAL PROCEDURE

The experiments were performed with a custom-built, Eiger style, ultrahigh-vacuum STM operated at 5 K.<sup>19</sup> The electronic properties of  $V_2O_3$  were deduced from differential conductance ( $dI/dV$ ) spectroscopy, performed with lock-in technique (bias modulation of 20 mV) and open feedback loop. The  $dI/dV$  spectra provide a measure of the LDOS in the oxide material. The size of the band gap, as deduced from the  $dI/dV$  spectra, is not corrected for band bending effects in the tip electric field, which are known to increase experimental gap sizes with respect to the flatband situation. Based on the bulk dielectric function and the anticipated de-

fect concentration in our  $V_2O_3$  films, this gap increase is estimated to be of the order of 100 meV.<sup>20</sup> Due to the large error bar in this approximation, we prefer to give the experimental values in the following as an upper limit of the actual gap size. Conductance imaging was performed to visualize the spatial distribution of the state density at a given energy.

The Au(111) sample was cleaned by repeated cycles of  $Ar^+$  sputtering (800 V and 10 mA) and annealing at 900 K. The oxide islands were prepared by reactive deposition of 5 ML (monolayer) vanadium onto Au(111) in an oxygen ambiance of  $1 \times 10^{-7}$  mbar at 300 K, followed by a short annealing to 600–700 K in ultrahigh vacuum.<sup>15,21–24</sup> The deposition rate of V was set to 1 ML/min. The described procedure results in the formation of hexagonally shaped, three-dimensional  $V_2O_3$  islands of 3–5 nm height, as revealed by low energy electron diffraction and STM measurements. The surface of vanadia islands is well ordered and covered with vanadyl ( $V=O$ ) groups.<sup>25–27</sup> In order to vary the bulk stoichiometry of  $V_2O_3$ , we performed more than 15 preparation cycles at different final annealing temperatures ranging between 600 and 700 K. Annealing to higher temperature hereby leads to the formation of oxygen-deficient vanadia (vanadium-rich  $V_2O_{3-x}$  phase), while lower annealing results in oxygen-rich structures with a large amount of vanadium vacancies (vanadium-poor  $V_{2-y}O_3$  phase). Previous experiments on non-stoichiometric  $V_{2-y}O_3$  demonstrated a preservation of the metallic phase even at low temperature.<sup>13,14</sup> We therefore expect a partial closing of the band gap when preparing the film outside the optimal temperature window to achieve stoichiometric samples.

In this paper, we will concentrate on  $V_2O_3$  thin films fabricated close to the optimum preparation conditions and only mention the trends observed for non-stoichiometric samples. The oxide composition is estimated from the size of the correlation band gap, determined to be 0.5–0.75 eV in the selected samples. This gap value is compatible with a concentration of V vacancies below 1%, as estimated from the following facts: (i)  $V_2O_3$  has naturally a small amount of V vacancies, (ii) the observed energy gap is close to the literature value of 0.6 eV for stoichiometric  $V_2O_3$ , and (iii) vacancy concentrations exceeding 5% induce a complete closing of the band gap in contrast to the experimental findings. Strongly overannealed vanadia films, on the other hand, exhibit a reduced gap size of 0.2–0.3 eV.

## RESULTS AND DISCUSSIONS

Figure 1 shows two STM topographic images of  $V_2O_3$  grown on Au(111). The overview image on the left displays two hexagonally shaped vanadium oxide islands on the reconstructed Au(111) surface. The atomic structure of the islands, not discernible in the large-scale scans, becomes visible as a hexagonal pattern with 4.95 Å lattice constant in the image shown on the right. In agreement with earlier studies, the bright protrusions are attributed to vanadyl ( $V=O$ ) groups, forming a  $(1 \times 1)$  structure on the oxide surface.<sup>22–26</sup> The vanadyl termination can be viewed as the  $O_3$  truncated bulk structure of  $V_2O_3$ , with one  $V=O$  group per unit cell adsorbed in a threefold hollow site. Density functional theory

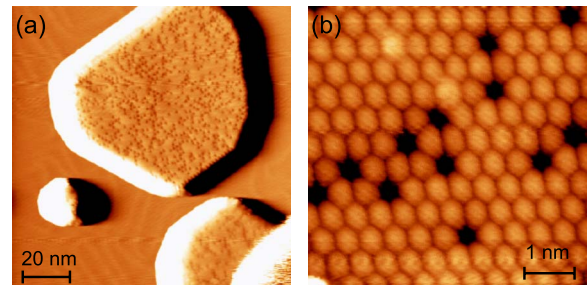


FIG. 1. (Color online) (a) STM image with two  $V_2O_3$  islands on Au(111). The tunneling parameters are  $U=1.2$  V and  $I=50$  pA. (b) High resolution STM image of a  $V_2O_3$  island showing the typical vanadyl termination with some point defects. Tunneling parameters are  $U=0.5$  V and  $I=50$  pA.

(DFT) calculations demonstrated that vanadyl-terminated  $V_2O_3$  (0001) has the lowest surface free energy and forms at oxygen chemical potentials that are typically used for vanadia preparation in an UHV system.<sup>27</sup> The depressions in the bright pattern of  $V=O$  groups are interpreted as defects, produced upon (partial) removal of the vanadyl species.

The surface topography of  $V_2O_3$  islands is nearly independent of the imaging conditions, e.g., bias voltage, polarity, and current, and always displays the hexagonal  $V=O$  network. Despite this well-ordered surface appearance, the electronic properties of the oxide film are rather inhomogeneous, as demonstrated by conductance imaging performed for different bias voltages and polarities. Large spatial variations in the  $dI/dV$  signal are discernable in these measurements, which occur at a length scale of about 1 nm and become most pronounced in images taken close to the band edges. A typical example is displayed in Figs. 2(a)–2(c), showing a topographic image of a  $V_2O_3$  island in combination with two conductance images taken at 240 and –240 mV. Variations in the  $dI/dV$  signal show up as contrast modulations, with bright and dark areas corresponding to high and low LDOS, respectively. The LDOS modulations reflect small shifts in the band edge positions at both sides of the correlation gap, as detailed further below. A comparison between topographic and conductance images in Fig. 2 demonstrates that areas with particularly high or low LDOS are not correlated with the positions of the  $V=O$  defects, although defects show a certain tendency to gather in regions with a lower density of unoccupied states (positive sample bias). This excludes an interpretation of the spatially modulated LDOS as being induced by surface defects, such as missing  $V=O$  groups. More likely, the conductance variations originate from the presence of bulk defects located in the region below the surface.

To investigate the electronic structure in more detail, we took  $dI/dV$  spectra along a line that connects two regions with different conductance behavior. Figures 2(d) and 2(e) show matrix representations of such spectral series taken along the arrows marked in Fig. 2(c). The spectral maps reveal a band gap of about 0.5 eV in a high-conductance region, while in regions with low  $dI/dV$  signal, the gap size increases to about 0.75 eV. Thus, gap variations of up to 50% occur on the length scale of 1–2 nm for this particular

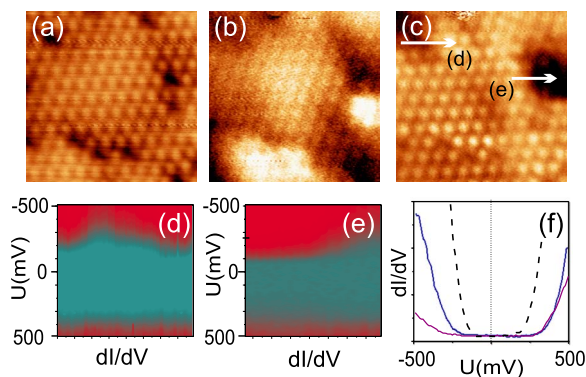


FIG. 2. (Color online) (a) STM topographic image of  $V_2O_3$  taken at 240 mV and 50 pA. Conductance images of the same region taken at (b) 240 mV and (c)  $-240$  mV. All images are  $5.5 \times 5.5$  nm<sup>2</sup> in size. The white arrows in (c) mark the course of the two spectral series shown in (d) and (e). In this matrix representation, turquoise color represents vanishing conductance and marks the correlation band gap, whereas red color corresponds to a high density of  $V_2O_3$  states. The flat structure of the conduction band edge is related to the positive set-point bias (500 mV and 100 pA) chosen for this spectral series, which causes a partial compensation of local conductance differences already by adjusting the tip height before spectral acquisition. (f) Two conductance spectra selected from (d) to visualize the gap size in regions with large (blue line) and small conductance (violet line). A spectrum taken on an overannealed film with strongly reduced gap size is shown for comparison (dashed line).

preparation. Figure 2(f) shows two representative spectra taken above a small-gap or large-gap region, respectively. The asymmetry of the band edge positions with respect to zero bias resembles a  $p$ -type conductance characteristic for this particular oxide region, as the Fermi level, fixed by the Au support, lies closer to the top of the valence band than to the bottom of the conduction band. Occasionally, also  $n$ -type regions are found on the surface with the Fermi level shifted toward the conduction band edge, as shown in Fig. 3(a). The maximum displacement of the Fermi level from the midgap position reaches  $\pm 20\%$  of the total gap size.<sup>28</sup>

Following the literature, a  $p$ -type characteristic in  $V_2O_3$  is the consequence of a finite concentration of V vacancies, which act as acceptor levels and introduce holes in the valence band. The corresponding local stoichiometry is formally described by  $V_{2-y}O_3$ .<sup>3</sup> The switching to a  $n$ -type behavior requires the presence of another defect type, which is assigned to oxygen vacancies here due to their general presence in transition metal oxides. Oxygen vacancies act as donors in  $V_2O_3$  and introduce electrons into the conduction band. The observed position of the Fermi level can, therefore, be used as a rough indicator for changes in the bulk stoichiometry of  $V_2O_3$  that decides on the dominance of either electrons or holes as majority carriers. Different hole concentrations in the oxide valence band are also responsible for changes in the band width and might contribute to the observed modulations of the gap size.<sup>8</sup> Due to compensation effects between acceptor and donor levels and missing information on their energy position in the gap, the local electron or hole concentration in the different oxide regions cannot be

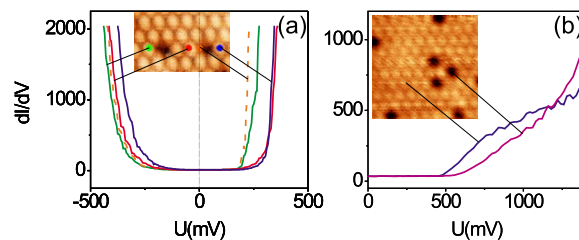


FIG. 3. (Color online) (a) Four  $dI/dV$  spectra taken on a vanadyl-terminated surface at the positions marked with the dots in the inset (color coded). The image size is  $1.5 \times 3$  nm<sup>2</sup>. In the green and orange curves, the Fermi level is slightly shifted toward the conduction band ( $n$ -type characteristic), whereas in the blue and red curves, it is shifted toward the valence band edge ( $p$ -type characteristics). For spectroscopic measurements, the tip was stabilized at  $-0.45$  V and 100 pA. (b)  $dI/dV$  spectra taken at a defect site (violet line) and above a  $V=O$  group (blue line). STM image is  $4.5 \times 4.5$  nm<sup>2</sup> in size. For spectroscopic measurements, the tip was stabilized at 1.4 V and 100 pA. The additional  $dI/dV$  intensity above the  $V=O$  lattice is attributed to a  $V=O$  related electronic state.

deduced from the  $dI/dV$  measurements. However, some general aspects shall be discussed in the following that may account for the shift of the Fermi level out of the midgap position.

A Fermi level position fixed by the temperature-dependent concentration of intrinsic  $V_2O_3$  carriers in the valence and conduction band is safely ruled out, as the large activation barrier for electron-hole excitations across the gap cannot be overcome at the measuring temperature of 5 K. Furthermore, intrinsic carriers are usually swamped by defect-induced ones in transition metal oxides, as very pure and stoichiometric samples are hard to produce and self-doping with cation or anion vacancies is extremely efficient. Also, a defect-induced behavior cannot account for the observed position of  $E_F$ . By considering only V vacancies in a simplified model, the associated acceptor levels will be separated from the valence band edge by the acceptor activation energy  $E_a$ . The trapping of electrons in those centers and the creation of holes in the valence band are then described by  $p \sim N_v \exp(-E_a/2kT)$ , with  $N_v$  the concentration of acceptor centers.<sup>12</sup> For strong compensation with donor levels, the hole concentration changes to  $p \sim N_v \exp(-E_a/kT)$ . In both cases, the Fermi level is pinned directly at or slightly below the acceptor level and will, therefore, be located close to the valence band edge, as observed in many semiconductors and oxide materials.<sup>12,29</sup> In analogy, a Fermi level pinned near the conduction band edge is expected if O vacancies would be the dominant defect type.<sup>29</sup> Both scenarios are in disagreement with the experimental observations, suggesting that self-doping of  $V_2O_3$  is not sufficient to explain the position of  $E_F$  close to gap center.

However, a moderate displacement of  $E_F$  from the midgap position can be rationalized when taking the influence of the Au support into account, which acts as an infinite electron reservoir and enables charge transport into and out of the oxide islands. In the case of  $p$ -like  $V_2O_3$ , the holes in the valence band are filled with electrons from Au(111), as de-



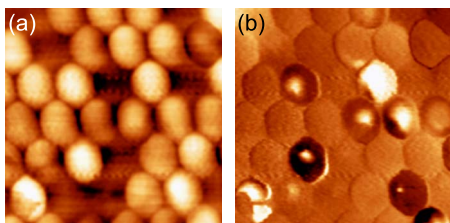


FIG. 4. (Color online) (a) STM and (b) corresponding conductance image taken at 200 mV and 50 pA. Both images are  $2.8 \times 2.8 \text{ nm}^2$  in size.

scribed with the formal configuration  $(\text{Au})^{\delta+}(\text{V}_{2-y}\text{O}_3)^{\delta-}$ . To compensate for the electron transfer, an electric field builds up between metal and oxide, inducing an upward bending of the oxide bands in response to the negative charge accumulated in the film. As a result, the Fermi level at the  $\text{V}_2\text{O}_3$  surface shifts from the midgap position toward the valence band edge. For  $n$ -conducting  $\text{V}_2\text{O}_3$ , electrons are transferred out of the oxide into the gold, leading to a situation described by  $(\text{Au})^{\delta-}(\text{V}_2\text{O}_{3-x})^{\delta+}$ . The oxide bands will bend downward and induce a shift of the Fermi level toward the conduction band edge in this case. A similar mechanism was earlier proposed to rationalize the unoccupied defect states occurring along line defects in alumina/ $\text{NiAl}(110)$ .<sup>30</sup> The  $\text{V}_2\text{O}_3$  film on  $\text{Au}(111)$  is, therefore, another example for the importance of the metal support in explaining the properties of a thin oxide film.<sup>31</sup>

In addition to bulk defects, also surface defects modify the local electronic structure of the  $\text{V}_2\text{O}_3$  islands. Their influence becomes apparent when comparing a  $dI/dV$  spectrum taken above a  $\text{V}=\text{O}$  group with one recorded above a vanadyl defect, as displayed in Fig. 3(b). The spectra reveal an additional  $dI/dV$  feature between 0.5 and 1.0 eV that appears exclusively above the  $\text{V}=\text{O}$  groups. The enhanced conductance is attributed to the presence of electronic states connected with the  $\text{V}=\text{O}$  termination. Vanadium atoms in  $\text{V}=\text{O}$  groups have an oxidation state of +5, which is typical for the  $\text{V}_2\text{O}_5$  oxide phase and does not occur in bulk  $\text{V}_2\text{O}_3$ . A higher oxidation state implies a partial emptying of the  $\text{V } 3d$  levels and an increase of the state density above the Fermi level, as observed experimentally. Recent DFT calculations showed that changes in the unoccupied LDOS mostly affect the vanadium  $t_{2g}$  and  $e_g$  orbitals in the  $\text{V}=\text{O}$  adlayer.<sup>27</sup> By comparing the calculated orbital energies with the experimental  $dI/dV$  feature, we suggest that mostly the  $e_g$  states contribute to the enhancement of the conductance above  $\text{V}=\text{O}$  groups.

Another peculiarity in the local electronic structure emerges in  $\text{V}_2\text{O}_3$  islands with a high density of missing vanadyl groups in the topmost layer (Fig. 4). While all  $\text{V}=\text{O}$  groups appear with similar contrast in the topographic image

shown in Fig. 4(a), they exhibit rather different  $dI/dV$  signals in the conductance map in Fig. 4(b). In particular, those  $\text{V}=\text{O}$  groups that are in contact with two and more defects are characterized by a clearly different  $dI/dV$  level compared to their neighbors. As the  $dI/dV$  map was taken close to the onset of the conduction band, slight shifts in the band edge could introduce large differences in the  $dI/dV$  signal. Such local changes in the edge position might result from pos./neg. excess charges localized at the surface as well as from the introduction or removal of electronic states at the band edge.<sup>32</sup> One possible explanation for the deviating behavior of  $\text{V}=\text{O}$  groups next to defect sites assumes that defects are not produced by a complete removal but by dissociation of the  $\text{V}=\text{O}$  group. The chemically unsaturated V atom remaining on the surface could then transfer charge to a neighboring  $\text{V}=\text{O}$  group, changing the oxidation state of its V ion. Oxygen detachment from the surface vanadyls is compatible with the fact that reduction of a  $\text{V}=\text{O}$  terminated surface via electron bombardment results in a V-terminated layer.<sup>26,33</sup> In a second model, the modified LDOS of isolated  $\text{V}=\text{O}$  groups might be induced by adsorbates. The most likely candidate is a H atom from the rest gas, given the high affinity of the vanadyl-terminated surface to form OH groups.<sup>34</sup> As  $\text{V}=\text{O}$  groups in direct contact with defects are more reactive than those inside a perfect layer, H adsorption will preferentially take place at those surface sites. The latter scenario is backed by the fact that modified vanadyls with unusual  $dI/dV$  signature sometimes hop to neighboring sites, as expected for the diffusive motion of an adsorbate. Both models would account for the observed contrast enhancement of  $\text{V}=\text{O}$  groups in direct contact to a defect. However, a discrimination exclusively on the basis of the STM measurements is not possible.

## CONCLUSIONS

The electronic structure of non-stoichiometric vanadium sesquioxide on  $\text{Au}(111)$  has been investigated by scanning tunneling microscopy and spectroscopy. The oxide islands are characterized by a pronounced band gap around the Fermi level that is assigned to the correlation gap of  $\text{V}_2\text{O}_3$  below the Mott transition. The gap size as well as the Fermi level position within the gap exhibit large spatial variations within the  $\text{V}_2\text{O}_3$  thin films. This inhomogeneity in the electronic structure is assigned to local deviations from the ideal oxide stoichiometry, causing fluctuations in the concentration of holes and excess electrons in valence and conduction bands, respectively. The position of the Fermi level in the gap is additionally modified by charge exchange with the  $\text{Au}(111)$  support. The ability of the  $\text{V}_2\text{O}_3$  to stabilize different stoichiometries on a nanometer length scale might be related to the high catalytic activity of this particular oxide material.

\*Corresponding author: nilius@fhi-berlin.mpg.de

- <sup>1</sup>B. Grzybowska-Swierkosz, F. Trifiro, and J. C. Vedrine, *Appl. Catal., A* **157**, 1 (1997).
- <sup>2</sup>S. Surnev, M. G. Ramsey, and F. P. Netzer, *Prog. Surf. Sci.* **73**, 117 (2003).
- <sup>3</sup>M. Imada, A. Fujimori, and Y. Tokura, *Rev. Mod. Phys.* **70**, 1039 (1998).
- <sup>4</sup>F. J. Morin, *Phys. Rev. Lett.* **3**, 34 (1959).
- <sup>5</sup>G. A. Thomas, D. H. Rapkine, S. A. Carter, A. J. Millis, T. F. Rosenbaum, P. Metcalf, and J. M. Honig, *Phys. Rev. Lett.* **73**, 1529 (1994).
- <sup>6</sup>M. Foex, *C. R. Acad. Sci. Hebd Seances Acad. Sci. D* **223**, 1126 (1946).
- <sup>7</sup>S. Shin, S. Suga, M. Taniguchi, M. Fujisawa, H. Kanzaki, A. Fujimori, H. Daimon, Y. Ueda, K. Kosuge, and S. Kachi, *Phys. Rev. B* **41**, 4993 (1990).
- <sup>8</sup>H.-D. Kim, H. Kumigashira, A. Ashihara, T. Takahashi, and Y. Ueda, *Phys. Rev. B* **57**, 1316 (1998).
- <sup>9</sup>A. Menth, A. C. Gossard, and J. P. Remeika, *J. Phys. (Paris), Colloq.* **1**, 1107 (1971); D. B. McWhan and J. P. Remeika, *Phys. Rev. B* **2**, 3734 (1970).
- <sup>10</sup>D. B. McWhan, A. Menth, J. P. Remeika, W. F. Brinkman, and T. M. Rice, *Phys. Rev. B* **7**, 1920 (1973).
- <sup>11</sup>Y. Ueda, K. Kosuge, and S. Kachi, *J. Solid State Chem.* **31**, 171 (1980).
- <sup>12</sup>P. A. Cox, *Transition Metal Oxides* (Oxford University Press, New York, 1992).
- <sup>13</sup>Y. Ueda, K. Kosuge, S. Kachi, T. Shinjo, and T. Takada, *Mater. Res. Bull.* **12**, 87 (1977).
- <sup>14</sup>Y. Ueda, K. Kosuge, S. Kachi, H. Yasuoka, H. Nishihara, and A. Heidemann, *J. Phys. Chem. Solids* **39**, 1281 (1978).
- <sup>15</sup>S. Guimond, M. Abu Haija, S. Kaya, J. Lu, J. Weissenrieder, S. K. Shaikhutdinov, H. Kühlenbeck, H.-J. Freund, J. Döbler, and J. Sauer, *Top. Catal.* **38**, 117 (2006).
- <sup>16</sup>B. Sass, C. Tusche, W. Felsch, N. Quaas, A. Weismann, and M. Wenderoth, *J. Phys.: Condens. Matter* **16**, 77 (2004).
- <sup>17</sup>O. Müller, J. P. Urbach, E. Goering, T. Weber, R. Barth, H. Schuler, M. Klemm, S. Horn, and M. L. denBoer, *Phys. Rev. B* **56**, 15056 (1997).
- <sup>18</sup>M. Preisinger, J. Will, M. Klemm, S. Klimm, and S. Horn, *Phys. Rev. B* **69**, 075423 (2004).
- <sup>19</sup>H.-P. Rust, J. Buisset, E. K. Schweizer, and L. Cramer, *Rev. Sci. Instrum.* **68**, 129 (1997).
- <sup>20</sup>R. M. Feenstra, *Phys. Rev. B* **50**, 4561 (1994); G. J. de Raad, D. M. Bruls, P. M. Koenraad, and J. H. Wolter, *ibid.* **66**, 195306 (2002).
- <sup>21</sup>F. P. Leisenberger, S. Surnev, L. Vitali, M. G. Ramsey, and F. P. Netzer, *J. Vac. Sci. Technol. A* **17**, 1743 (1999).
- <sup>22</sup>S. Surnev, G. Kresse, M. G. Ramsey, and F. P. Netzer, *Phys. Rev. Lett.* **87**, 086102 (2001); S. Surnev, G. Kresse, M. Sock, M. G. Ramsey, and F. P. Netzer, *Surf. Sci.* **495**, 91 (2001).
- <sup>23</sup>M. Abu Haija, S. Guimond, A. Uhl, H. Kühlenbeck, H.-J. Freund, J. K. Todorova, M. V. Ganduglia-Pirovano, J. Döbler, and J. Sauer, *Surf. Sci.* **600**, 1497 (2006).
- <sup>24</sup>J. Schoiswohl, M. Sock, S. Surnev, M. G. Ramsey, F. P. Netzer, G. Kresse, and J. N. Andersen, *Surf. Sci.* **555**, 101 (2004).
- <sup>25</sup>S. Surnev, L. Vitali, M. G. Ramsey, F. P. Netzer, G. Kresse, and J. Hafner, *Phys. Rev. B* **61**, 13945 (2000).
- <sup>26</sup>A. C. Dupuis, M. Abu Haija, B. Richter, H. Kühlenbeck, and H.-J. Freund, *Surf. Sci.* **539**, 99 (2003).
- <sup>27</sup>G. Kresse, S. Surnev, J. Schoiswohl, and F. P. Netzer, *Surf. Sci.* **555**, 118 (2004).
- <sup>28</sup>The Fermi level position in the vanadia band gap is affected by the Schottky barrier at the metal-oxide interface. The work function difference between pristine  $V_2O_3$  and Au(111) suggests a downward bending of the oxide bands. The size of this effect depends on the atomic nature of the Au- $V_2O_3$  interface, the presence of charged interface states, and the oxide defect concentration, and cannot be quantified at this point. We expect, however, a nonlocal influence on the Fermi level position, providing an offset on the spatial variations observed in the conductance behavior.
- <sup>29</sup>U. Diebold, *Surf. Sci. Rep.* **48**, 53 (2003).
- <sup>30</sup>M. Schmid, M. Shishkin, G. Kresse, E. Napetschnig, P. Varga, M. Kulawik, N. Nilius, H. P. Rust, and H. J. Freund, *Phys. Rev. Lett.* **97**, 046101 (2006).
- <sup>31</sup>H. J. Freund, *Surf. Sci.* **601**, 1438 (2007).
- <sup>32</sup>M. Batzill, K. Katsiev, D. J. Gaspar, and U. Diebold, *Phys. Rev. B* **66**, 235401 (2002).
- <sup>33</sup>J. Schoiswohl, S. Surnev, M. Sock, S. Eck, M. G. Ramsey, F. P. Netzer, and G. Kresse, *Phys. Rev. B* **71**, 165437 (2005).
- <sup>34</sup>B. Tepper, B. Richter, A.-C. Dupuis, H. Kühlenbeck, C. Hucho, P. Schilbe, M. A. bin Yarmo, and H.-J. Freund, *Surf. Sci.* **496**, 64 (2002).